Formation of a TiO_2 Micronetwork on a UV-Absorbing SiO_2-Based Glass Surface by Excimer Laser Irradiation

Aiko Narazaki,*,† Yoshizo Kawaguchi,† Hiroyuki Niino,† Masanori Shojiya,‡ Hirotaka Koyo,‡ and Keiji Tsunetomo‡

Photonics Research Institute, National Institute of Advanced Industrial Science and Technology (AIST), Tsukuba Central 5, Higashi 1-1-1, Tsukuba, Ibaraki 305-8565, Japan, and Technical Research Laboratory, Kansai Research Center, Nippon Sheet Glass Co., Ltd., 1, Kaidoshita, Konoike, Itami, Hyogo 664-8520, Japan

Received August 16, 2005. Revised Manuscript Received October 20, 2005

We report on the preparation of TiO_2 micronetworks on a UV-absorbing $Na_2O-TiO_2-SiO_2$ glass surface by excimer laser irradiation, a technique we have called laser-induced superficial phase separation. The TiO_2 micronetworks that were formed on the etched glass surface were in the rutile crystalline phase and exhibited a photocatalytic capability. We were also able to form a range of TiO_2 micronetworks in an array of 20-μm holes. This flexible formation of photocatalytic TiO_2 networks on a glass surface without any heat treatments could enable a new route for developing novel microdevices, such as monolithic microfluidics with light-catalyzed reactions and miniaturized solar batteries.

Introduction

Etching of SiO_2-based glass materials has been studied extensively for a wide array of uses, such as micro-optics, microelectromechanical systems (MEMS), and bionanotechnology applications, because these materials are transparent over a wide spectral range and exhibit high durability to elevated temperatures, humidity, and chemicals.[1−5] Common etching methods include reactive ion etching (RIE), plasma etching, and wet chemical etching, which have usually been used for microfabrication in combination with photolithography. So far, these techniques have mainly been developed with the aim of achieving a smooth etched surface. However, when etched glass surfaces are used as flow channels in the MEMS process, they might also need to include smaller structures peculiar to the particular applications, such as micropillars and micropores for mixing fluids, supporting catalysts, and so forth. The ability to form such nano- and micro-sized structures through lithography-free etching processes is still uncommon, but this technology has begun to attract increasing attention as a unique and simple route for microfabrication. Zeze et al. reported the preparation of submicron quartz columns with a high aspect ratio by utilizing the lithography-free RIE of quartz.[1] They suggested that differential etching occurred between the glass column and the underlying surface as a result of localized metallic impurities and a nonuniform distribution of the electrostatic fields, leading to the nonuniform appearance of these particular columns.

On the other hand, excimer laser etching utilizing a mask-projection system is potentially valuable as a simple, resist-free process for microfabrication.[6−8] However, the application of laser etching to SiO_2-based glasses is difficult because they exhibit very low absorption of laser light. To overcome this obstacle, SiO_2-based glasses containing a controlled quantity of TiO_2 (hereafter known as UV-absorbing glass) have been developed by Nippon Sheet Glass Co., Ltd.; the addition of TiO_2 induces strong absorption, but only in the UV region.[9] When this UV-absorbing glass is exposed to a KrF excimer laser, we found that the formation of a TiO_2 micronetwork occurs simultaneously with the etching of the other constituents of the glass, which we term laser-induced superficial phase separation. It is well-known that TiO_2 is a material that has shown promising photocatalytic and optoelectronic conversion abilities in the crystalline phase, which has accelerated its development for various integration techniques.[10−13] We also confirmed that the TiO_2 micronetworks were precipitated in the rutile crystalline phase and that they exhibited photocatalytic capability. This is, to our best knowledge, the first report of the formation of crystalline

* To whom correspondence should be addressed. Tel.: +81-29-861-4564. Fax: +81-29-861-4560. E-mail: aiko-narazaki@aist.go.jp.
† National Institute of Advanced Industrial Science and Technology (AIST).
‡ Nippon Sheet Glass Co., Ltd.

(1) Zeze, D. A.; Cox, D. C.; Weiss, B. L.; Silva, S. R. P. *Appl. Phys. Lett.* **2004**, *84*, 1362.
(2) Choi, D. Y.; Lee, J. H.; Kim, D. S.; Jung, S. T. *J. Appl. Phys.* **2004**, *95*, 8400.
(3) Kobayashi, J.; Mori, Y.; Okamoto, K.; Akiyama, R.; Ueno, M.; Kitamori, T.; Kobayashi, S. *Science* **2004**, *304*, 1305.
(4) Yamakawa, K.; Hori, M.; Goto, T.; Den, S.; Katagiri, T.; Kano, H. *Appl. Phys. Lett.* **2004**, *85*, 549.
(5) Lee, K. B.; Lin, L. *Sens. Actuators A* **2004**, *111*, 44.
(6) Bäuerle, D. *Laser Processing and Chemistry*, 3rd ed.; Springer: Berlin, 2000.
(7) Ding, X.; Kawaguchi, Y.; Sato, T.; Narazaki, A.; Niino, H. *Langmuir* **2004**, *20*, 9769.
(8) Höche, T.; Böhme, R.; Gerlach, J. W.; Frost, F.; Zimmer, K.; Rauschenbach, B. *Nano Lett.* **2004**, *4*, 895.
(9) Koyo, H.; Shojiya, M.; Tsunetomo, K. *Proc. SPIE* **2004**, *5662*, 40.
(10) Xiang, J.; Masuda, Y.; Koumoto, K. *Adv. Mater.* **2004**, *16*, 1461.
(11) Gao, Y.; Masuda Y.; Koumoto, K. *Chem. Mater.* **2004**, *16*, 1062.
(12) Kotani, Y.; Matsuda, A.; Kogure, T.; Tatsumisago, M.; Minami, T. *Chem. Mater.* **2001**, *13*, 2144.
(13) Caruso, R. A.; Antonietti, M.; Giersig, M.; Hentze, H.-P.; Jia, J. *Chem. Mater.* **2001**, *13*, 1114.

10.1021/cm0518372 CCC: $30.25
Published on Web 12/01/2005

TiO_2 micronetworks on glass surfaces without the application of any heat treatments and/or adhesives.

Experimental Section

$Na_2O-TiO_2-SiO_2$ glass (Nippon Sheet Glass) sheets were used as UV-absorbing SiO_2-based glass samples. This glass has been developed as a UV laser-machinable glass that absorbs light in the UV range. The TiO_2 compositions used in this study were 5, 30 and 40 mol %. X-ray diffraction measurements confirmed that the original glasses were fully amorphous. Using a transmission electron microscope (TEM; Topcon, EM-002B), original glasses thinned by a focused ion beam method were also observed. As a result, there were no phase-separation-derived structures such as nanosized particles, indicating that the original glasses were uniformly amorphous. On the other hand, with over 40 mol % TiO_2, it was difficult to maintain a uniform amorphous state. To etch the sample surface, KrF excimer laser pulses (Lambda Physik, EMG-MSC201; $\lambda = 248$ nm, fwhm ≈ 30 ns) were accumulated through a beam homogenizer onto a glass surface at 5 Hz under flowing helium gas.

Top and cross-sectional observations of the laser-irradiated glass surface were performed with a scanning electron microscope (SEM; Keyence, VE-7800). Observations with a confocal scanning laser microscope (Keyence, VK-8500) provided information about the surface morphology. The crystalline structure was examined by micro-Raman spectroscopy at a spatial resolution of 1 μm (JASCO, NRS-1000) using the second-harmonic wave of a CW Nd:YAG laser operated at 15 mW as an excitation source. To investigate the distribution of the constituents of the glass, electron probe microanalysis (EPMA) measurements were also carried out using a JEOL JXA-8200 system. Distribution maps for both titanium and silicon were measured using wavelength-dispersive X-ray analysis (WDX), and sodium was detected by energy-dispersive X-ray (EDX) analysis (JEOL, JXA733) to avoid the diffusion of sodium during the measurements.

The photocatalytic performance of the laser-irradiated glass surface was also evaluated because it was found that the surface modification with rutile TiO_2 micronetworks occurred after the KrF excimer laser irradiation. The photocatalytic ability was tested with respect to photocatalytic decomposition of methylene blue (MB) contacted with the glass surface. A 10 μmol/L MB solution in a resin cell of 35 mL was placed on the sample glass surface and kept in the dark for 120 min to saturate the absorption of MB onto the surface. The cell was capped with a glass cover to eliminate the influence of O_3 produced by UV-lamp irradiation of air. Then, the solution was exposed to the irradiation from a black light lamp (Toshiba Lighting & Technology, FL20S-BLB). The light intensity of the UV lamp at the position of the sample was set at 1 mW cm^{-2}. The photodegradation of MB as a function of exposure time was monitored using a spectrophotometer (Perkin-Elmer, Lambda900).

Results and Discussion

Figure 1a shows a top-view SEM image of a micronetwork structure prepared by KrF excimer laser irradiation of a UV-absorbing $Na_2O-TiO_2-SiO_2$ glass with 30 mol % TiO_2. An accumulation of 500 laser pulses at a fluence of 0.6 J·cm^{-2} was applied under flowing helium gas, resulting in the formation of a micronetwork on the surface, which had been etched to a depth of about 10 μm. The micronetwork was reproducible in the case of both glasses containing 30 and 40 mol % TiO_2. On the other hand, instead of the micronetwork, submicron islands were observed under the same irradiation condition for a glass with 5 mol % of TiO_2. On the basis of these results, we determined that a high concentration of TiO_2 is vital for the formation of a continuous micronetwork. Hereafter, we will concentrate on this unique laser-induced micronetwork structure and show results on glasses with a TiO_2 concentration of 30 mol %.

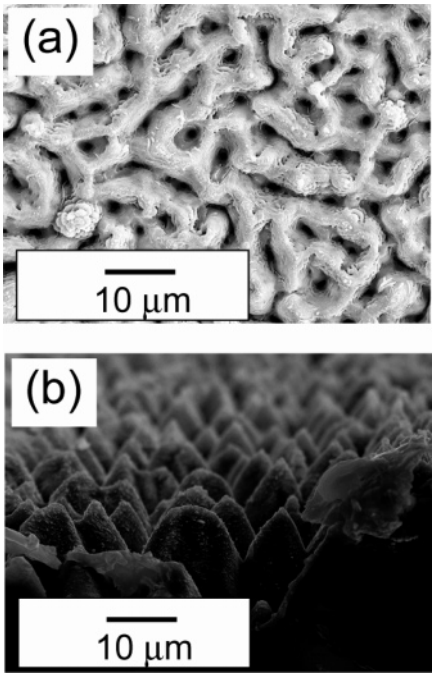

Figure 1. (a) Top- and (b) cross-sectional-view SEM micrographs of micronetwork structures prepared by KrF excimer laser irradiation on a UV-absorbing glass surface. The laser fluence and number of pulses were set at 0.6 J·cm^{-2} and 500 pulses, respectively.

The formation of the micronetworks also depended strongly on the laser fluence; the networks were observed only over a narrow fluence range, from the ablation threshold of 0.2 to 0.6 J·cm^{-2}, whereas the etched surface became smoother above 0.8 J·cm^{-2}. The presence of the gas flow was important for the formation of the micronetwork. In addition to helium, the micronetwork was formed by laser irradiation under flowing nitrogen gas, although it was observed that some of the concave parts of the network were filled. On the other hand, we could not fabricate micronetwork structures by laser irradiation without gas flow over the entire fluence range employed in this work. Judging from these results, it is probable that the gas flow helps to remove ablated species from the concave parts of the micronetwork. The incomplete micronetwork structure prepared under the nitrogen gas flow might come from shorter mean free path, that is, less removal ability. Figure 1b shows a cross-sectional SEM image of the sample etched at 0.6 J·cm^{-2}. This observation confirmed that a continuous network was formed by the conjunction of many cones with a height of ca. 9 μm. Hence, the application of laser irradiation in order to etch the surface of a UV-absorbing glass caused the simultaneous generation of a micronetwork.

Micro-Raman spectroscopic measurements were performed on the glass surface without and with laser irradiation. Figure 2a,b shows the micro-Raman spectra of a glass before irradiation and the micronetwork formed after irradiation,

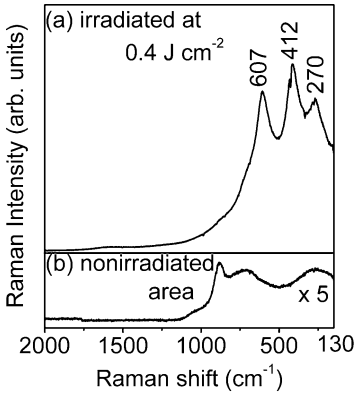

Figure 2. Micro-Raman spectra of (a) a micronetwork and (b) a nonirradiated glass surface. The micronetwork was fabricated by the accumulation of 500 laser pulses at 0.4 J·cm^{-2}. The numbers in the figure represent the wavenumbers of the Raman peaks. The Raman peaks from the laser-induced micronetwork that appear at 412 and 607 cm^{-1} can be assigned to TiO_2 in the rutile crystalline phase.

respectively. Because the second-harmonic wave of a Nd:YAG laser with a beam diameter of 1 μm was used as the excitation source, the spatial resolution of the measurement was about 1 μm. In the case of the spectrum from the micronetwork, the excitation beam was focused on the skeleton of a continuous network. As a result, three intense peaks appeared at 270, 412, and 607 cm^{-1}, whereas no intense peaks were observed from the virgin glass surface. The Raman peaks at 412 and 607 cm^{-1} can be assigned to crystalline TiO_2 in the rutile phase. The rutile phase has four Raman-active modes and exhibits two strong Raman peaks at 448 cm^{-1} (E_g) and 613 cm^{-1} (A_{1g}) with two other weak peaks at 144 cm^{-1} (B_{1g}) and 827 cm^{-1} (B_{2g}).[14,15] Here, it should be mentioned that the peaks observed at 412 and 607 cm^{-1} show red shifts from the literature data of 448 and 613 cm^{-1}, respectively, and such spectral modifications might be caused by an oxygen deficiency. In fact, a red shift of the rutile E_g line to 424 cm^{-1} was reported for a TiO_2 sample prepared by a gas condensation method.[16] The recovery in the peak position toward 448 cm^{-1} was observed after the sample had been annealed at elevated temperatures in air, whereas annealing in argon did not change the peak position. Thus, they concluded that the oxygen deficiency might lead to the shifting of Raman lines. Moreover, they mentioned that the rutile E_g mode (448 cm^{-1}) was more sensitive to this oxygen deficiency than the A_{1g} mode (613 cm^{-1}), which corresponds with our results that the 448 cm^{-1} band is shifted farther than the 613 cm^{-1} band. The relatively broad peak at approximately 270 cm^{-1} is still unassigned but might be the result of a defect-induced disorder in relation to the oxygen deficiency or a second-order process. On the other hand, six Raman-active modes exist for the anatase phase, so the most intense peak would be recorded at 144 cm^{-1} (E_g) in addition to other peaks at 197 cm^{-1} (E_g), 397 cm^{-1} (B_{1g}), 518 cm^{-1} (A_{1g} and B_{1g}, unresolved), and 640 cm^{-1} (E_g).[14,15] Therefore, we can conclude that the micronetwork was composed of TiO_2 rutile crystallites.

(14) Robert, T. D.; Laude, L. D.; Geskin, V. M.; Lazzaroni, R.; Gouttebaron, R. *Thin Solid Films* **2003**, *440*, 268.
(15) Iwabuchi, A.; Choo, C.; Tanaka, K. *J. Phys. Chem. B* **2004**, *108*, 10863.
(16) Parker, J. C.; Siegel, R. W. *J. Mater. Res.* **1990**, *5*, 1246.

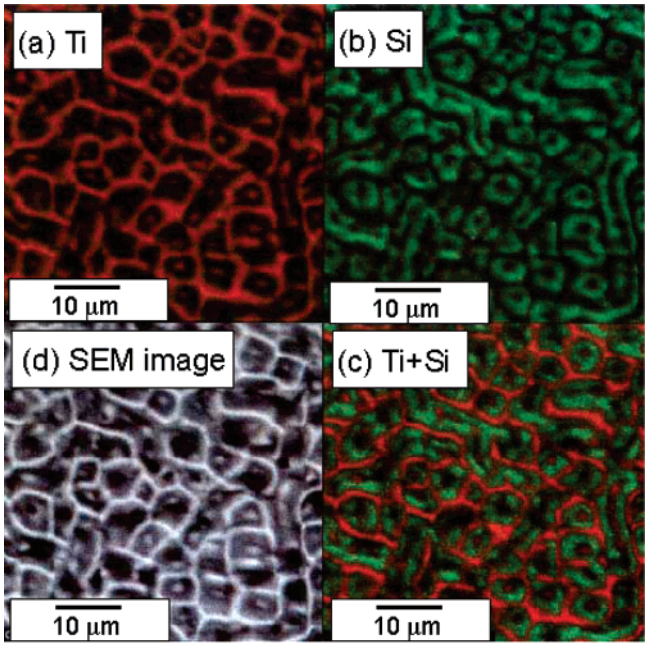

Figure 3. EPMA maps of (a) titanium, (b) silicon, and (c) a combination of titanium and silicon. The color gradation from green to red corresponds to the relative concentration of the titanium and silicon, respectively; a more intense color represents a higher concentration. (d) SEM image composed of reflected electrons. The EPMA maps show that the titanium is mainly distributed on the micronetwork, whereas the silicon mainly appears in the concave parts around the network.

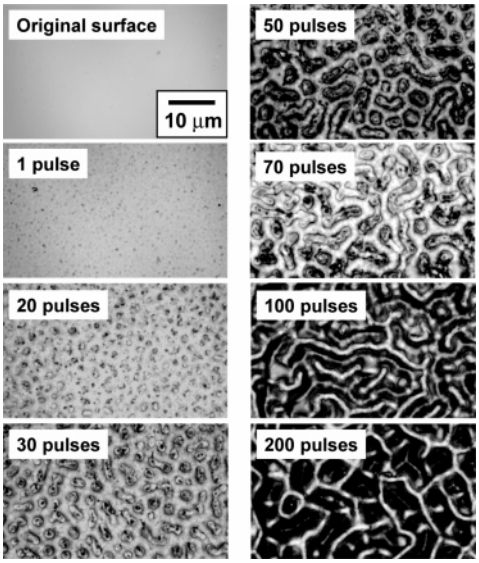

Figure 4. Structural evolution as a function of number of laser pulses. The laser fluence was 0.3 J·cm^{-2}. Small bumps appeared after the first pulse, which then grew to microcones with a diameter of 1−2 μm and a height of ca. 0.3 μm after 20 pulses. The cones started to conjoin after 200 pulses, resulting in a TiO_2 (rutile) micronetwork with a height of 3 μm.

Figure 3 shows typical EPMA maps and an SEM image composed of reflected electrons for an etched glass surface with a TiO_2 micronetwork. The green-to-red color gradation seen in Figure 3a−c corresponds to the relative concentrations of titanium and silicon, respectively; the more intense color indicates a higher concentration. The EPMA maps show the distribution of titanium in the micronetwork, whereas silicon appears mainly in the concave parts around the network. Thus, a nonuniform distribution of titanium and silicon (i.e., phase separation between TiO_2 and SiO_2) was induced by the laser irradiation. Moreover, the UV-absorbing

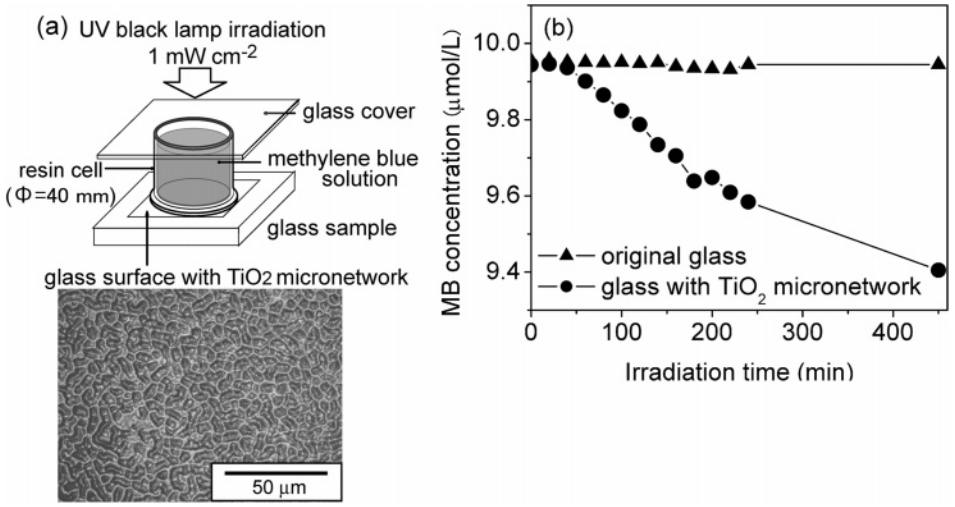

Figure 5. (a) Basic experimental setup adopted in studying the photocatalytic properties of a laser-induced TiO_2 micronetwork. A glass surface with the TiO_2 micronetwork was contacted with methylene blue (MB) solution under UV illumination from a black lamp. (b) Change in MB concentration due to the photocatalytic decomposition by the TiO_2 micronetwork as a function of UV-lamp irradiation time (solid circles). As a reference, an original glass surface was subjected to the same experiment (solid triangles).

glass originally contains a certain level of alkaline oxide. According to the EPMA analysis for the alkali element (not shown), the alkali concentration diminished in both the TiO_2 micronetwork and the underlying SiO_2-rich surface, indicating that the composition on the laser-irradiated surface became closer to a TiO_2-SiO_2 binary system. From these results, it can be said that the TiO_2 micronetwork was formed as a result of the laser-induced phase separation into TiO_2- and SiO_2-rich phases, followed by selective etching of the SiO_2-rich phase.

The formation of the micronetworks was remarkably dependent on the laser fluence: at fluences higher than 0.8 $J \cdot cm^{-2}$, the etch rate dramatically increased, and the etched surface became smooth. The Raman spectrum of this smooth surface was similar with that of the virgin glass surface shown in Figure 2b, indicating no precipitation of the TiO_2 crystalline phase. This might be because the micronetwork is obliterated when the fluence is much higher than the ablation threshold, leading to a smooth etched surface. In other words, we were able to control the morphology of the etched surface and could produce either a flat surface or one modified with a TiO_2 micronetwork.

For the purposes of studying the formation mechanism of the TiO_2 micronetwork, we investigated the dependence of the morphology on the number of laser pulses. Figure 4 shows a series of confocal scanning laser microscopic images of a glass surface as a function of the number of laser pulses that were applied to it. Small bumps appeared after the first pulse, which then grew into microcones with a diameter of 1−2 μm and a height of ca. 0.3 μm after 20 pulses. The cones then started to converge, resulting in a TiO_2 (rutile) micronetwork with a height of 3 μm after 200 pulses. This kind of structural evolution with accumulating laser pulses is strongly analogous to the phase-separation textures prepared by rapid quenching of a TiO_2-SiO_2 melt; with an increase in the TiO_2 volume fraction, the texture changes from binodal-type isolated particles to a spinodal-type continuous structure.[17] On the basis of this analogy, one possible mechanism for this is as follows. A nanosecond laser

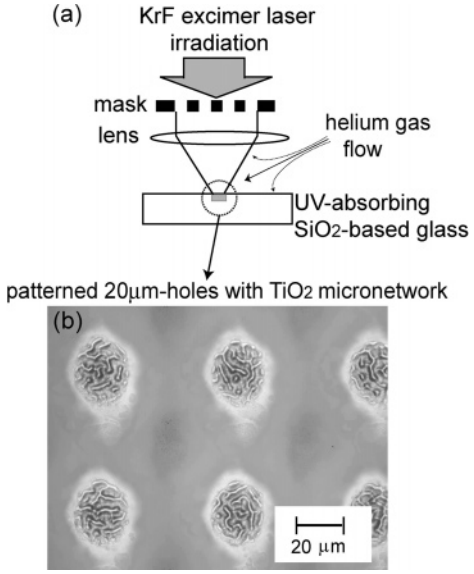

Figure 6. (a) Schematic of the setup used for laser microfabrication with a mask-projection system. The mask was composed of an array of holes that had a projected diameter of 20 μm on a glass surface. (b) Confocal scanning laser microscopic image of patterned 20-μm holes. The formation of a TiO_2 micronetwork was observed at the bottom of the 20-μm holes, as seen in Figure 1a in the case of large-area irradiation.

pulse instantaneously raises the surface temperature, thereby ablating the constituents of the glass. Because alkali oxide has a higher vapor pressure than TiO_2 and SiO_2, the alkali oxide tends to evaporate more easily, causing a compositional shift toward a TiO_2-SiO_2 binary system at the etched surface. According to the phase diagram reported for the TiO_2-SiO_2 system,[18] the immiscibility region has a wide range from ca. 20 to 90 mass % TiO_2 above 1780 °C, resulting in two liquids. Below this temperature, the system is composed of the rutile crystalline phase and a SiO_2-rich melt.[18] In consequence, a larger fraction of the SiO_2-rich

(17) Katsumata, K.; Kameshima, Y.; Okada, K.; Yasumori, A. *Mater. Res. Bull.* **2004**, *39*, 1131.
(18) Devries, R. C.; Roy, R.; Osbron, F. F. *Trans. Br. Ceram. Soc.* **1954**, *59*, 525.

phase evaporates during cooling, resulting in the formation of TiO_2 bumps. As the number of laser pulses accumulates, the TiO_2 bumps grow and begin to connect to each other, resulting in the formation of the TiO_2 micronetwork.

TiO_2-based materials have been widely considered as the most promising photocatalysts because of their excellent photoreactivity, nontoxicity, and long-term stability. Using our newly developed method, we are able to create TiO_2 micronetworks directly on a UV-absorbing glass surface by UV laser irradiation without the application of any heat treatments and/or adhesives. To evaluate the photocatalytic performance of the thus-obtained TiO_2 micronetworks, the decomposition of methylene blue (MB) via TiO_2-mediated photoreaction was studied, as shown in Figure 5a. Figure 5b shows the change in MB concentration as a function of lamp exposure time. The solid circles denote the data in the case of existence of TiO_2 micronetwork prepared by the irradiation of 200 KrF excimer laser pulses at 0.5 $J \cdot cm^{-2}$. The solid triangles correspond to an original glass surface without the laser treatment. Compared to the absence of a change for the original glass, the laser-treated glass obviously decreased the MB concentration, indicating that the laser-induced TiO_2 micronetwork exhibits a photocatalytic ability.

Finally, we demonstrate the formation of a TiO_2 micronetwork in the bottom of a 20-μm hole array microfabricated by KrF excimer laser irradiation with a mask-projection system, as shown in Figure 6a. Figure 6b shows a confocal scanning laser microscopic image of an array of holes. A micronetwork was observed at the bottom of each hole, indicating that a flexible arrangement of TiO_2 micronetworks (applicable to the modification of microfluidics, for instance) can be achieved by utilizing this technique.

Conclusions

A TiO_2 micronetwork in the rutile crystalline phase was fabricated via excimer laser irradiation of UV-absorbing $Na_2O-TiO_2-SiO_2$ glasses. A glass surface with the TiO_2 micronetwork exhibits a photocatalytic capability. An arrangement of TiO_2 micronetworks in an array of 20-μm holes was also achieved by laser microfabrication with a mask-projection system. Such flexible arrangements of photocatalytic micronetworks seem promising for the modification of microdevices with TiO_2 such as for monolithic microfluidics with a light-catalyzed reaction.

CM0518372